Available online at www.sciencedirect.com
ScienceDirect
Plant Physiology and Biochemistry 46 (2008) 309–324
Plant Physiology and Biochemistry
www.elsevier.com/locate/plaphy

Review

Structure and mechanism of inhibition of plant acetohydroxyacid synthase

Ronald G. Duggleby [a,*], Jennifer A. McCourt [a], Luke W. Guddat [b]

[a] RDBiotech, 22 Parklands Boulevard, Little Mountain, Queensland 4551, Australia
[b] School of Molecular and Microbial Sciences, University of Queensland, Brisbane, Queensland 4072, Australia

Received 27 August 2007
Available online 14 January 2008

Abstract

Plants and microorganisms synthesize valine, leucine and isoleucine via a common pathway in which the first reaction is catalysed by acetohydroxyacid synthase (AHAS, EC 2.2.1.6). This enzyme is of substantial importance because it is the target of several herbicides, including all members of the popular sulfonylurea and imidazolinone families. However, the emergence of resistant weeds due to mutations that interfere with the inhibition of AHAS is now a worldwide problem. Here we summarize recent ideas on the way in which these herbicides inhibit the enzyme, based on the 3D structure of *Arabidopsis thaliana* AHAS. This structure also reveals important clues for understanding how various mutations can lead to herbicide resistance.

Keywords: Acetohydroxyacid synthase; Branched-chain amino acids; Herbicide; Inhibitor; Protein structure; Herbicide resistance

1. Branched-chain amino acid synthesis

Most plants synthesise all of their organic constituents from CO_2. Therefore they must contain a full complement of biosynthetic pathways and their component enzymes. Microorganisms may use pre-existing compounds from their environment, such as simple sugars and organic acids, as the starting point for biosynthesis but they still must perform a large variety of biochemical transformations. In contrast, animals have complex dietary requirements due to their inability to make various fats, amino acids, vitamins and so on. The branched-chain amino acids are an example.

Valine, leucine and isoleucine are essential in the diet of animals while plants and microorganisms synthesise the carbon skeletons of these amino acids from pyruvate alone (valine synthesis), pyruvate plus acetyl-CoA (leucine) or pyruvate plus 2-ketobutyrate (isoleucine). This metabolic pathway is illustrated in Fig. 1A. The first step in this process, in which either 2-acetolactate (AL) or 2-aceto-2-hydroxybutyrate (AHB) is formed, is catalysed by acetohydroxyacid synthase (AHAS, EC 2.2.1.6). In the older literature AHAS is often called acetolactate synthase but this name is not preferred because it ignores the role of the enzyme in AHB synthesis. The name acetolactate synthase (ALS) should be reserved for a different enzyme that produces AL only, such as that found in *Klebsiella pneumoniae* [49]. Plant biochemists have been rather slow to adopt this modern and more correct nomenclature.

AHAS activity is not present in animals but it has been detected in all plants where measurements have been attempted. In microorganisms, an open reading frame consistent with AHAS has been identified in most of the large number of genomes that have been sequenced. The best characterised AHASs are the three isoenzymes found in *Escherichia coli*. In this article we focus on the three-dimensional structure of

Abbreviations: AHAS, acetohydroxyacid synthase; AHB, 2-aceto-2-hydroxybutyrate; AL, 2-acetolactate; ALS, acetolactate synthase; CE, chlorimuron ethyl; CoA, coenzyme A; CS, chlorsulfuron; FAD, flavin adenine dinucleotide; $FADH_2$, reduced FAD; IP, imazapyr; IQ, imazaquin; IT, imazethapyr; MM, metsulfuron methyl; PDB, Protein Databank; SM, sulfometuron methyl; TB, tribenuron methyl; ThDP, thiamine diphosphate.

* Corresponding author. Tel.: +61 7 5491 3037.
E-mail address: ron_duggleby@fastmail.com.au (R.G. Duggleby).

0981-9428/$ - see front matter © 2007 Elsevier Masson SAS. All rights reserved.
doi:10.1016/j.plaphy.2007.12.004

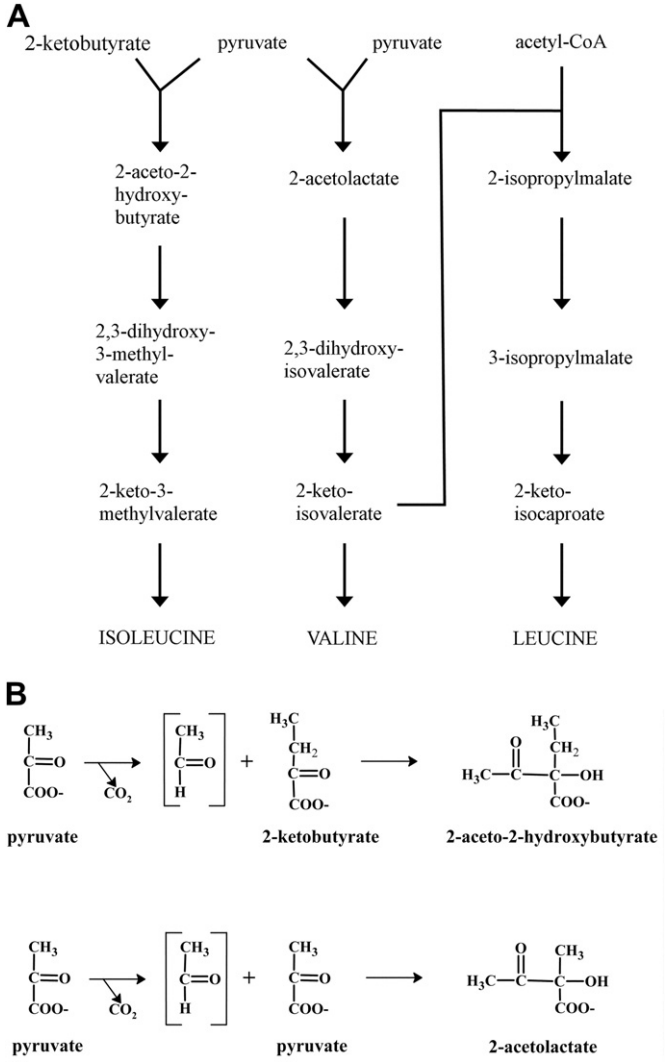

Fig. 1. Reactions of branched-chain amino acid biosynthesis. (A) Isoleucine is formed in four enzyme-catalysed steps, starting with 2-ketobutyrate and pyruvate. Valine is formed by a parallel pathway with a second molecule of pyruvate replacing 2-ketobutyrate. Leucine is formed by a four-step extension of the valine pathway, with the first reaction combining 2-ketoisovalerate with acetyl-CoA. (B) In the reactions catalysed by AHAS, enzyme-bound ThDP reacts with pyruvate, releasing CO_2 and forming an acetaldehyde moiety as enzyme-bound hydroxyethyl-ThDP. This resonating enamine/α-carbanion intermediate then reacts with 2-ketobutyrate (upper panel) or pyruvate (lower panel) to form AHB or AL, respectively.

the enzyme with particular emphasis on the recently published structure of the catalytic subunit of AHAS from *Arabidopsis thaliana* [41]. To put the importance of the structure in perspective, we first give a brief overview of the properties of AHAS. The reader is referred to two recent reviews [7,38] for more extensive accounts of the occurrence, role, properties, structure and catalytic mechanism of AHAS.

2. Properties of AHAS

2.1. Reactions and mechanism of AHAS

As indicated in Fig. 1A, AHAS catalyses two very similar reactions and these are shown in more detail in Fig. 1B. In the branch of the pathway leading to isoleucine, a molecule of pyruvate undergoes decarboxylation to yield an enzyme-bound acetaldehyde moiety that reacts with 2-ketobutyrate yielding AHB. In the branch leading to valine and leucine, 2-ketobutyrate is replaced by pyruvate, forming AL. The first stage in each case is reminiscent of the reactions catalysed by a large family of enzymes where there is cleavage of a carbon–carbon bond adjacent to a carbonyl group [10]. This family of enzymes all require thiamine diphosphate (ThDP) as an essential cofactor, and AHAS is no exception. ThDP reacts with pyruvate, releasing CO_2 and forming enzyme-bound hydroxyethyl-ThDP as a resonating enamine/α-carbanion intermediate. This then reacts with the 2-ketoacid acceptor (2-ketobutyrate or pyruvate) to form the corresponding acetohydroxyacid (AHB or AL). It will be evident that 2-ketobutyrate and pyruvate compete for the intermediate and it is observed for most forms of AHAS that there is a marked preference for the former. This preference neatly compensates for the fact that intracellular concentrations are markedly in favour of pyruvate, resulting in similar fluxes down the two branches of the pathway.

Like all members of this ThDP-dependent family of enzymes, ThDP is anchored in the active site by a divalent metal ion cofactor such as Mg^{2+}. Unlike most other members of the family, AHAS requires flavin adenine dinucleotide (FAD) as a third cofactor. Until recently, the function of FAD was puzzling because the reaction catalysed involves no oxidation or reduction. It is now clear that the presence of FAD in AHAS is an evolutionary relic of the ancestry of its sub-family of ThDP-dependent enzymes [10].

2.2. Feedback inhibition of AHAS

AHAS catalyses the first step leading to all three branched-chain amino acids. As might be anticipated, it is regulated by these end products. For bacterial and fungal AHAS this regulation is mediated mainly, and usually solely, through valine inhibition. The plant enzyme is inhibited by each of the branched-chain amino acids with similar potency but leucine acts synergistically with either valine or isoleucine. For example, *A. thaliana* AHAS has inhibition constants for leucine and valine of 336 and 231 μM, respectively, but a K_i of 12.3 μM for an equimolar mixture of the two [34].

2.3. AHAS subunits

The enzyme is composed of two types of subunit. One of them contains ThDP, is usually active alone and is designated the catalytic subunit. It has a molecular mass in the 59–66 kDa range although in eukaryotes it is synthesised as a larger precursor protein. An N-terminal peptide, which is subsequently removed, is required to direct the protein to mitochondria in fungi and to chloroplasts in plants. The second subunit possesses no AHAS activity but greatly stimulates the activity of the catalytic subunit. This second subunit is necessary for AHAS to be inhibited by branched-chain amino acids and is therefore designated as the regulatory subunit. The molecular mass of this regulatory subunit varies greatly

across species. In bacteria it is usually quite small and generally ranges between 10 and 20 kDa. In eukaryotes it is larger; 34 kDa in yeast [46] and over 50 kDa in plants [22,34]. It is also synthesised as a larger precursor protein with an N-terminal organelle-targeting peptide. The catalytic and regulatory subunits were formerly called the large and small subunits, respectively. This was before the discovery of the eukaryotic versions of the regulatory subunit, which approach the size of the catalytic subunit. This older usage should therefore be discouraged.

The structures of the catalytic subunit from yeast [40,48,51] and *A. thaliana* [41] have been determined. Discussion of these is deferred until Section 3. The first regulatory subunit structure to be published [26] (PDB code 2F1F) was for one of the three isoenzymes (AHASIII) found in *E. coli*. The protein is a dimer (Fig. 2), with each 18.1 kDa monomer containing two βαββαβ ferredoxin-like domains of similar size. Confirming an earlier prediction [42], the two 76-residue N-terminal domains (Fig. 2, foreground) assemble to form a structure similar to the regulatory domain of 3-phosphoglycerate dehydrogenase. Based on the effect of mutations in weakening feedback inhibition, the location of the valine-binding sites was proposed to be in the interface between this pair of domains (Fig. 2, arrows). Very recently the crystal structures of two orthologues of this regulatory subunit, one from *Thermotoga maritima* and the other from *Nitrosomonas europa*, have been reported [53]. These two proteins both have a very similar overall fold to that of the regulatory subunit of *E. coli* AHASIII and all three proteins contain a bound divalent metal ion (Mg^{2+} or Ca^{2+}). However, the position of this metal ion differs in the *E. coli* protein and it is unclear whether these binding sites are of any physiological relevance. These structures offer few clues about where the subunit interfaces with the catalytic subunit, how association activates the enzyme, or how valine binding to the regulatory subunit inhibits AHAS activity.

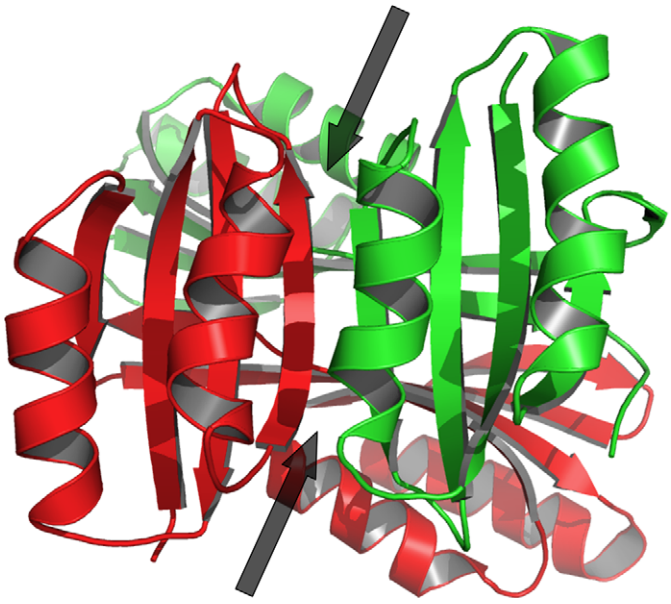

Fig. 2. Structure of the regulatory subunit of *E. coli* AHAS isoenzyme III. The protein is a dimer of two identical 18.1 kDa monomers (shown in red and green) with each containing two domains of similar size. The proposed locations of the valine-binding sites (arrows) are at the interface between the pair of N-terminal domains (foreground).

All AHAS regulatory subunit amino acid sequences contain a homologue of the N-terminal domain and most also contain a homologue of the C-terminal domain. In addition to this common core of approximately 140 residues, the protein from yeast and other fungi is larger due to an insert of 38–55 residues. This insert has been shown [35] to be responsible for a unique property of fungal AHAS: the inhibition by valine is reversed by MgATP [47]. The plant AHAS regulatory subunit is larger still, because it contains two copies of the 140-residue core. Bearing in mind the synergistic inhibition between leucine and valine/isoleucine, this structure invites the speculation that the duplicate regions provide two separate regulatory sites, one for leucine and one for valine/isoleucine. Reconstitution studies of the *A. thaliana* AHAS catalytic subunit with the two separate repeats of its regulatory subunit support this proposal [34].

2.4. Herbicidal AHAS inhibitors

Major interest in AHAS developed when the sulfonylurea herbicides were discovered [36]. At the time, their mode of action was unknown and it was not until 1984 that it was shown that these compounds inhibit bacterial [29] and plant [4,55] AHAS. Simultaneously and independently, the imidazolinone herbicides were also found to be AHAS inhibitors [59]. The discovery that AHAS is the target also helped to explain why these herbicides have very low toxicity in animals: the enzyme is absent from animals so toxicity could only arise if there were unrelated processes affected by these compounds. Knowing that AHAS inhibitors are effective and safe herbicides has led to the development of several other chemically-distinct compounds such as the sulfonylaminocarbonyltriazolinones, the triazolopyrimidines and the pyrimidyl(oxy/thio)benzoates (see [38], for structures) that have been used commercially. Structures of two examples of sulfonylurea (chlorimuron ethyl (CE) and metsulfuron methyl (MM)) and imidazolinone (imazapyr (IP) and imazaquin (IQ)) herbicides are shown in Fig. 3.

The typical sulfonylureas have a central bridge with an *ortho*-substituted aromatic ring attached to the sulfur atom and a heterocyclic ring, disubstituted in both *meta* positions, attached to the distal nitrogen atom of the sulfonylurea bridge. This heterocycle can be a pyrimidine (as in CE) or a triazine (MM). Modifications to the sulfonylurea bridge greatly diminish herbicidal activity and the potency of AHAS inhibition [68]. The imidazolinones all have a methyl and an isopropyl substituent on the dihydroimidazolinone ring, generating an asymmetric centre. The two isomers differ by about 10-fold in their activity [63]. The other substituent is an aromatic, and usually heterocyclic, ring with a carboxylate in the *ortho* position.

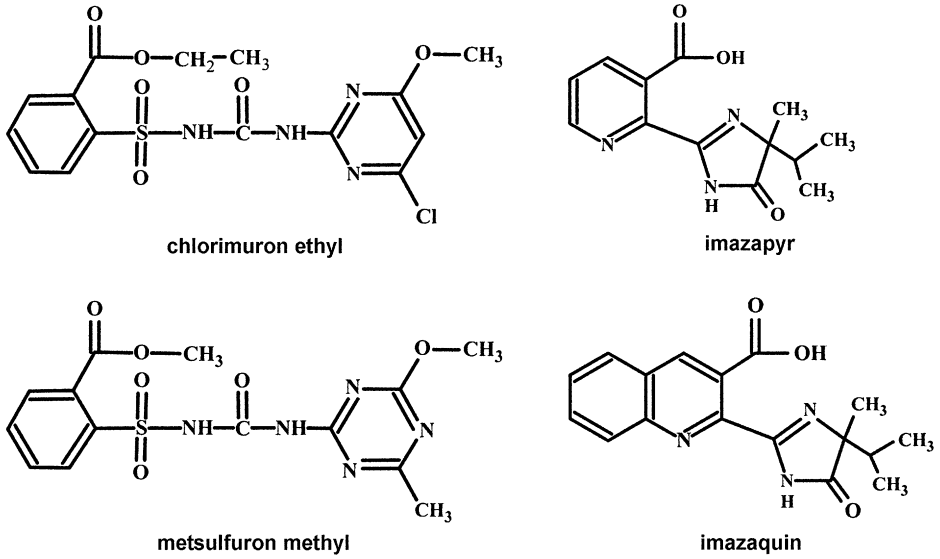

Fig. 3. Structures of typical sulfonylurea and imidazolinone herbicides. Chlorimuron ethyl and metsulfuron methyl are sulfonylureas while imazapyr and imazaquin are imidazolinones.

The inhibition of AHAS by both sulfonylureas and imidazolinones is complex. An important contributor to this complexity is that the inhibition is time-dependent. There is an initial weak inhibition over the first few minutes that becomes progressively stronger with time. The usual assay for AHAS activity [62] involves incubation for a set period of time in the range 10 min to 2 h, followed by a colorimetric measurement of total product formation over this period. Therefore, the calculated activity is an average of the changing activity over the period of the assay. As a result, many of the published inhibition constants, including some of our own measurements, must be regarded as approximations only. The description of the initial inhibition as "weak" needs to be qualified; for the *A. thaliana* enzyme, where the initial inhibition has been measured accurately [6] using a continuous assay [58], the K_i is 3 μM for IQ and 11 nM for CE. As a rule of thumb, sulfonylureas are approximately 100-times more potent as AHAS inhibitors than the imidazolinones. Curiously, the recommended field application rates of the two classes are similar (e.g. ~50 g/hectare for both CE and IQ). Although herbicidal activity depends ultimately upon inhibition of AHAS, the differences between the *in vivo* and *in vitro* potencies of these compounds are undoubtedly due to a combination of physical barriers between the site of application and the intracellular target, degradation and detoxification by the plant, and stability in the soil.

For *in vitro* studies, the very low K_i values for the sulfonylureas may be comparable to the enzyme concentration used in the assay, meaning that tight-binding effects will occur. In tight-binding inhibition, the free concentration of the inhibitor is diminished by binding to the enzyme and this complication is often not taken into account when calculating K_i values. Fortunately the colorimetric assay is extremely sensitive so that very low enzyme concentrations can be employed, where tight-binding effects will be of minor importance. For the much less sensitive continuous assay, tight-binding inhibition may dominate.

The reversibility of the inhibition is unclear and the results obtained by various workers depend on the conditions used when incubating the enzyme with the herbicide, the source of the enzyme, the nature of the herbicide, and the method used in attempts to regenerate activity. Our interpretation of the variety of results obtained is that binding of the herbicide induces progressive damage to the ThDP cofactor, particularly when catalysis is taking place. This neatly explains why the inhibition is time-dependent. Activity will be regenerated, at least partially, if conditions allow replacement of the damaged cofactor with fresh ThDP. Damage to ThDP in AHAS, even in the absence of herbicides, has been demonstrated directly [39] and this damage occurs more rapidly during turnover.

The inhibition by these herbicides is noncompetitive or uncompetitive with pyruvate [5]. Measuring the inhibition at a single substrate only, as is usually the case, will yield an apparent inhibition constant that depends on the pyruvate concentration and its K_m. Therefore, comparisons between measurements in different laboratories may not be reliable. Even when experimental conditions are identical, comparing the K_i for AHAS from different sources, or between wild-type and mutants from a single species, may not be strictly valid if the K_m value of the compared enzymes differs. The fact that the inhibition is not competitive has been interpreted [29] to mean that these herbicides bind preferentially (though perhaps not exclusively) to the enzyme-bound hydroxyethyl-ThDP intermediate.

The sulfonylurea and imidazolinone herbicides were developed without realising that they were targeting AHAS, let alone with any knowledge of the molecular architecture of their binding site on the enzyme. From their structures alone, it would have been impossible to predict that they would be powerful inhibitors of AHAS. Once their target was identified,

speculations arose as to how they inhibit the enzyme. There is no similarity between these herbicides and the substrate or product, so binding to the active site appeared to be unlikely. Moreover, there are superficial similarities only between sulfonylureas and imidazolinones and any shared structural elements are also found in a vast range of compounds that do not inhibit AHAS, suggesting that they may act at independent sites. The identification of AHAS variants that are insensitive to one or both families (see Section 4.2) led to the idea that they bind to different, but overlapping, sites.

Little progress was made in understanding the structure of the herbicide-binding site(s) because crystallisation of the enzyme remained elusive. Various models have been constructed based on homology with the related enzyme pyruvate oxidase [11,23,24,45] but these models have proved to be of limited value because the predicted location of the herbicide-binding site and the orientation of the herbicide was highly speculative at the time.

We decided to address this problem and in 2002 we solved the crystal structure of yeast AHAS [48]. Later we determined this structure with several bound sulfonylureas [40,51] allowing for the first time visualisation of the precise location of the site where these herbicides bind. More recently, we solved the crystal structure of *A. thaliana* AHAS with several sulfonylureas and with one of the imidazolinones [41]. These structures now allow us to see precisely the nature and differences between sulfonylurea- and imidazolinone-binding sites. In Sections 3 and 4, these structures are described. Later we describe how these structures have allowed us to understand how AHAS mutations give rise to herbicide resistance.

3. X-ray structures of AHAS

The first crystal structure determined for an AHAS from any source was that of the catalytic subunit from the yeast, *Saccharomyces cerevisiae* [48]. In view of the fact that the enzyme is an established target for herbicides, it may seem odd that this non-plant AHAS was chosen for crystal structure determination. The explanation is that crystallization trials of the *A. thaliana* protein were undertaken initially but these proved to be unsuccessful. In these experiments the plasmid constructs encoded the mature protein only, which was obtained in relatively small yields after purification. However, initial crystallization trials of the catalytic subunit of *S. cerevisiae* AHAS were undertaken using a construct that encoded the mature protein with a hexahistidine tag at the N-terminal end [50]. This allowed large quantities of this enzyme to be purified quickly and facilitated crystallization. Subsequently, a version of the plant AHAS incorporating a hexahistidine tag (at the C-terminus) was constructed and crystallization of this enzyme became possible [52].

The crystal structure of the catalytic subunit of yeast AHAS (PDB code 1JSC) was determined to 2.6 Å resolution [48]. It revealed the overall fold of the enzyme and the location of the three cofactors, ThDP, Mg^{2+} and FAD within the active site. To date, this structure remains as the only AHAS from any source that has been crystallized successfully as the herbicide-free enzyme. This initial study was followed up by structures of this subunit in complex with the sulfonylurea herbicide, CE [51] (1N0H) and then by structures of this enzyme in complex with four other sulfonylureas [40]: MM (1T9D), chlorsulfuron (CS, 1T9B), sulfometuron methyl (SM, 1T9C) and tribenuron methyl (TB, 1T9A). The resolution of the diffraction data for these herbicide–AHAS complexes varies between 2.2 Å for the CS-bound structure to 2.8 Å for the CE-bound structure. Despite numerous attempts our group, and possibly others, has failed to obtain high resolution diffraction data for any member of the imidazolinone family of herbicides in complex with the yeast enzyme. The best data that could be measured for any such complex was to 3.8 Å resolution, which is not sufficient to resolve the location of this herbicide, or even reveal whether the imidazolinone is actually present in the crystal.

More recently, the crystal structure of the catalytic subunit of *A. thaliana* AHAS was determined in complex with CE (1YBH), CS (1YHZ), MM (1YHY), SM (1YI0), TB (1YI1) and with IQ (1Z8N), the first structure with a member of the imidazolinone family [41]. Diffraction data for these structures were in the 2.5–2.9 Å range. Attempts to crystallize this plant enzyme in complex with the regulatory subunit or in the absence of an herbicide have met with no success. Thus, for *A. thaliana* AHAS, comparisons between the binding mode of the imidazolinone and sulfonylurea herbicide families can be made (see later) but no comparative analysis of herbicide-free and herbicide-bound enzyme can be conducted.

3.1. Overall structure of the catalytic subunit of plant AHAS

A. thaliana AHAS in the presence of any of the sulfonylurea herbicides or IQ crystallizes as a tetramer (Fig. 4A) with a overall subunit arrangement similar to that observed for other ThDP-dependent enzymes including pyruvate oxidase [43], pyruvate decarboxylase [14], benzoylformate decarboxylase [17] and ALS [49]. Finding this tetramer is somewhat surprising because in gel filtration studies, *A. thaliana* AHAS elutes at a molecular mass of ~110 kDa showing that in solution the catalytic subunit exists as a dimer [5]. However, when the complex between the regulatory and catalytic subunits of the enzyme is formed it has an apparent mass of ~500 kDa suggesting that there are four regulatory and four catalytic subunits in the assembly [34]. It appears that the AHAS catalytic subunit tetramer is favoured at the high concentrations of the protein needed for crystallization, or as a consequence of crystallization.

Each polypeptide of the catalytic subunit of *A. thaliana* AHAS consists of three domains (Fig. 4B), α (residues 86–280), β (residues 281–451) and γ (residues 463–639) with each having a similar overall fold of a six-stranded parallel β-sheet surrounded by six to nine helices (Fig. 5). Note that the numbering of the polypeptide starts at 86 because the DNA encoding the putative 85 residue chloroplast transit peptide was removed during cloning. In the α-domain, the six-stranded β-sheet is flanked by the helices numbered 1, 2 and

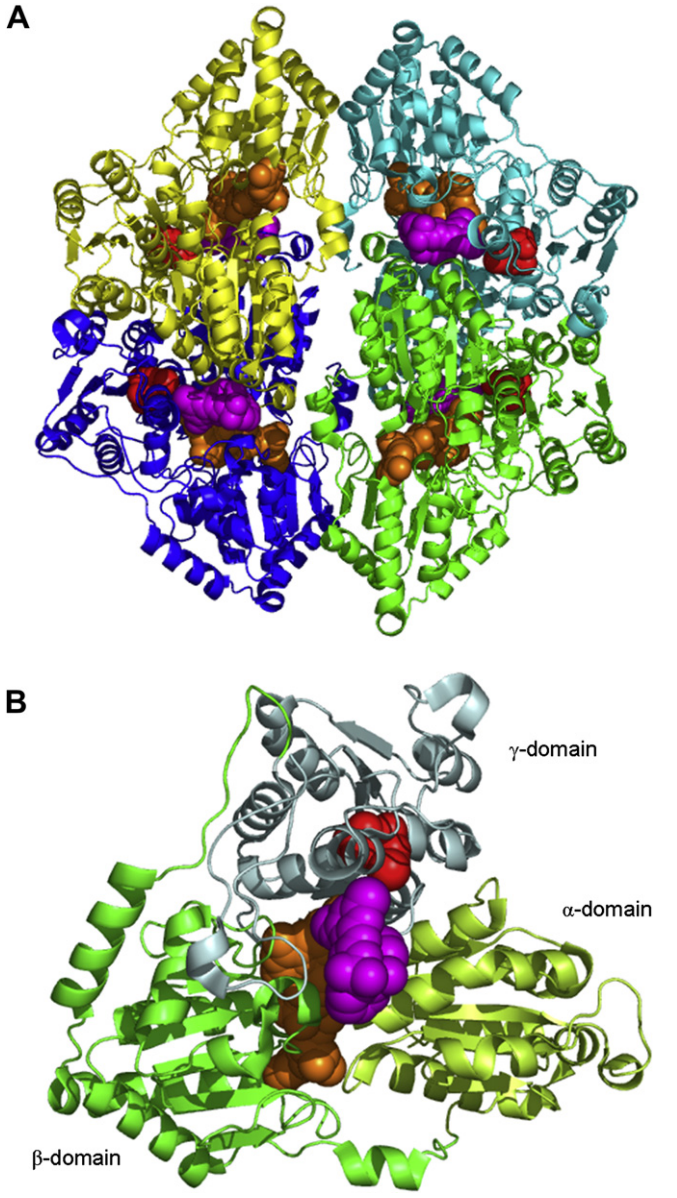

Fig. 4. Structure of the *A. thaliana* AHAS catalytic subunit in complex with the herbicide CE. (A) Overall structure of the tetramer. Each subunit is coloured differently with FAD, CE and ethyl dihydrogen phosphate (a breakdown product of ThDP) depicted as orange, magenta and red coloured spheres, respectively. (B) Structure of an individual catalytic subunit of *A. thaliana* AHAS. The colour scheme is as for Fig. 4A except that the α-, β- and γ-domains are coloured lime green, bright green and grey-green respectively.

7 on one face and helices 3, 4, and 6 on the opposite face (Fig. 5). Two smaller helices, 5 and 8, are located orthogonal to and at the C-terminal end of the major β-sheet. Two additional short anti-parallel β-strands are also observed in this domain. One is at the N-terminus, which includes residues 97–98, and the other is towards the C-terminus of the domain, which includes residues 262–263. This β-sheet is stabilized by two polypeptide backbone hydrogen bonds between R97 and A263. Helix 9 (residues 273–278) is also assigned to the α-domain but its function is to link to the β-domain rather than being in the core of the α-domain.

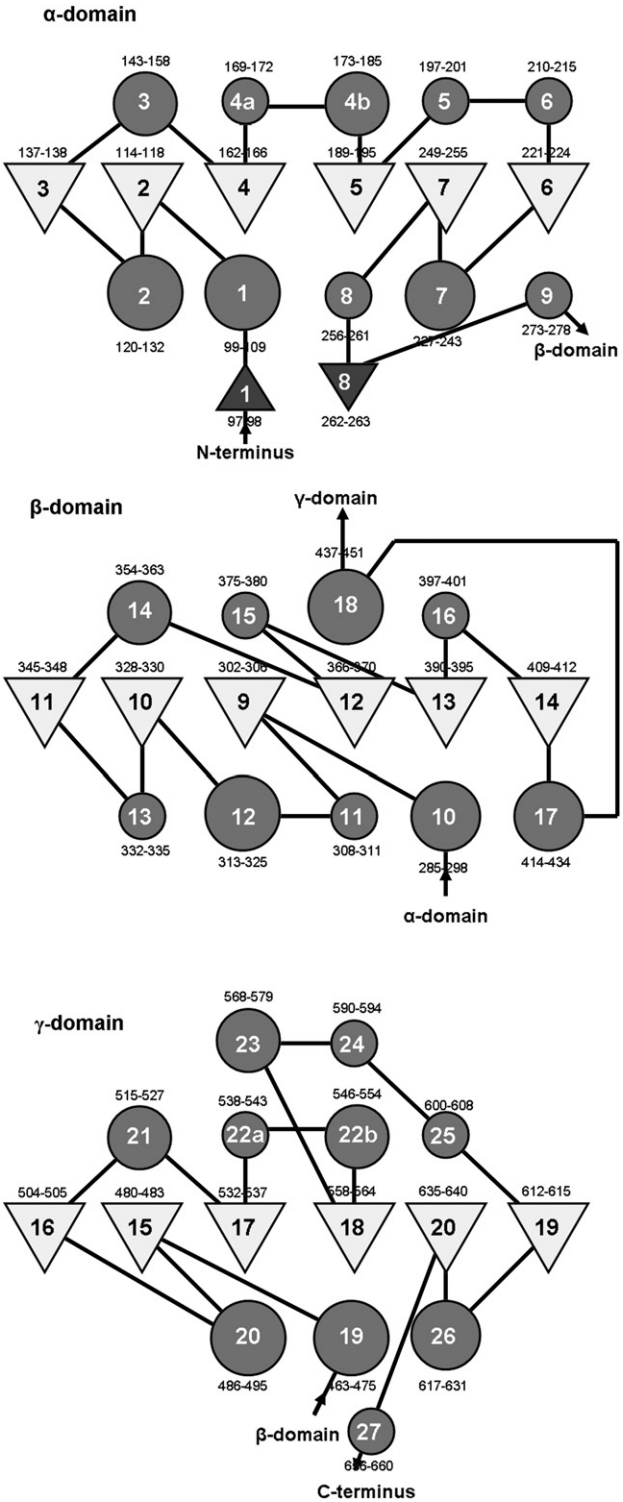

Fig. 5. Two-dimensional topology diagram of the *A. thaliana* AHAS catalytic subunit using the coordinates of the complex with IQ. α-Helices are shown as circles and β-strands as triangles (light shading for the six-stranded core β-sheet). The triangles point in the same direction for parallel β-strands and in opposite directions for antiparallel β-strands. Helix 4 has a kink in it and is therefore shown as two sections, 4a and 4b. Helix 22 is shown as two sections for the same reason.

The β-domain also has a central six-stranded parallel β-sheet but the topology is distinctly different from that of the α-domain [10]. Helices 10, 12 and 17 are together on one face of the sheet and helices 14, 15 and 18 are on the opposite face. Three short helices, 11, 13 and 16, are the only other secondary elements present in this domain.

The γ-domain has the same underlying topology as the α-domain but is slightly simpler in structure. Again, a six-stranded sheet is central to this domain, which is flanked on one face by helices 21, 22 and 25 and by helices 19, 20 and 26 on the other face. Helix 23, which includes 568–579, is located parallel to the six stranded β-sheet, but as an extension to the C-terminal end rather than in a flanking position. This helix is surrounded by polypeptide that is essentially random coil except for two short helices, 24 (residues 590–594) and 27 (residues 656–660).

3.2. Active site of AHAS

The catalytic subunit of AHAS requires three cofactors for activity, ThDP, Mg^{2+} and FAD. The most important for the catalytic mechanism is ThDP; its C2 atom initiates catalysis and therefore defines the centre of the active site. Each tetramer of the catalytic subunit of *A. thaliana* AHAS has four active sites (Fig. 4A). Each active site is at the interface of two monomers; hence the minimal requirement for AHAS activity is a dimer of the catalytic subunits. The biological relevance of the tetramers is unclear; they may make the enzyme more stable, or enable the regulatory subunits to bind more efficiently.

In all of the crystal structures of *A. thaliana* AHAS determined to date the active site is completely buried, making it unclear as to how substrate can gain direct access. No crystal structure has been determined for a plant AHAS as the free enzyme or in the presence of a substrate, intermediate or product. However, our studies on the catalytic subunit of yeast AHAS, where we have structures in the presence and absence of herbicide, give clues about how substrate can enter. In comparing these yeast AHAS structures (Fig. 6) two regions of polypeptide become ordered when herbicide is bound. One segment is residues 580–595 and the other is residues 650–687, constituting the final 38 C-terminal residues of the polypeptide. The region between 580 and 595 forms part of a wall of the herbicide-binding site (see later) and interacts directly with the disubstituted pyrimidine or triazine ring. In particular, W586 forms a π-stacking arrangement with this ring. Mutagenesis of this residue results in a 6250-fold reduction in sensitivity for CE [12], and in plants the equivalent residue (W574) is the most commonly observed resistance mutation site (see Section 4.2). Thus, in the free enzyme, this wall is not present, allowing the active site to be exposed to solvent and therefore accessible to substrate. None of the 38 residues of the C-terminal tail directly interact with the herbicide in this yeast AHAS structure. The closest approach is for G657 which is ∼5 Å from the oxygen of the sulfonyl group of CE. Nonetheless the region of the polypeptide between V655 and S659 also forms part of the wall leading to the active site in the herbicide-bound structure (Fig. 6). We therefore hypothesize that in the free structure and in solution these two regions are quite flexible allowing substrate relatively easy access. Upon substrate binding this region becomes ordered with the active site shielded from solvent during catalysis. It is likely that the regulatory subunit plays a significant role in ordering the active site during catalysis. Unfortunately, there are currently no structures available of the catalytic subunit in combination with the regulatory subunit to probe the effect of this interaction on the active site.

3.3. ThDP-binding site

ThDP is central to the active site. However, in all of the structures of the catalytic subunit of *A. thaliana* AHAS where a sulfonylurea is bound, much of the electron density for this cofactor is incomplete. Typically, portions of the thiazolium ring near to and including the sulfur atom are missing. In more extreme cases the complete thiazolium ring and parts of the pyrimidine ring are missing. However, the diphosphate region is present in all of the structures. Interestingly, ThDP is observed as the complete cofactor in the *A. thaliana* AHAS

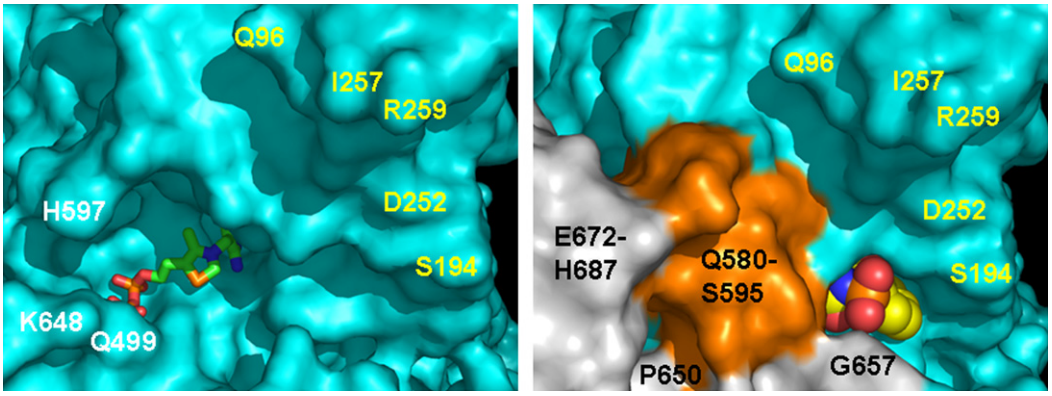

Fig. 6. Comparison of the structure of the catalytic subunit of yeast AHAS before (left) and after (right) herbicide binding. Prior to herbicide binding ThDP (shown as a stick model on the left) is exposed to the solvent. After herbicide binding, the orange region (580–595) and the grey region (650–687) become ordered burying ThDP and residues such as Q499, H597 and K648. The solid spheres in the right image represent the sulfonylurea (CE) protruding from the top of the tunnel created by the ordering of the residues coloured in orange and grey.

complex with IQ, and also in the free yeast AHAS structure but is again broken down in the yeast AHAS structures where any of the sulfonylureas are bound. Thus, the degradation of ThDP appears to occur or be accelerated as a consequence of sulfonylurea binding. It is known that bonds containing sulfur are susceptible to damage in response to exposure by X-rays [3] and also that ThDP is intrinsically unstable when bound to AHAS [39] or other ThDP dependent enzymes [1,9]. It is therefore hypothesized that upon sulfonylurea binding and closure of the active site, the carbanion of ThDP can form leading to its subsequent degradation [40]. As mentioned earlier, a similar process in the presence of substrate accounts for the time-dependence of herbicide inhibition.

Where there is electron density to show the complete structure of ThDP (i.e. IQ-bound *A. thaliana* AHAS (Fig. 7) and herbicide-free yeast AHAS) the pyrimidine and thiazolium rings adopt a V conformation. The angle between the C5′ and C7′ atom of the pyrimidine ring and the N3 atom of the thiazolium ring best defines this V shape. In the herbicide-free yeast AHAS and IQ-bound *A. thaliana* AHAS structures this angle is 112° and 113°, respectively. This conformation is strongly influenced by a methionine side-chain which protrudes out of the surface of the polypeptide to force the bend (Fig. 7). Two values that further describe the relationship between these two rings are Φ_T (the dihedral angle between C4′, C5′, C7′ and N3) and Φ_P (the dihedral angle between C5′, C7′, N3 and C2). In both pyruvate decarboxylase [14] and yeast AHAS [48] the values for these angles are 96° and −66°. However, in *A. thaliana* AHAS with bound IQ these dihedral angles are 104° and −61° respectively. The variation in these dihedral angles appears to be influenced by the region between 568 and 583 in *A. thaliana* AHAS (580–595 in yeast AHAS numbering), which is ordered and helical in *A. thaliana* AHAS but disordered in yeast AHAS. Of particular note is the side-chain of L568 in *A. thaliana* AHAS which would be only 2.9 Å from the C6 atom of ThDP if this cofactor adopted the same conformation as observed in the herbicide-free yeast AHAS structure.

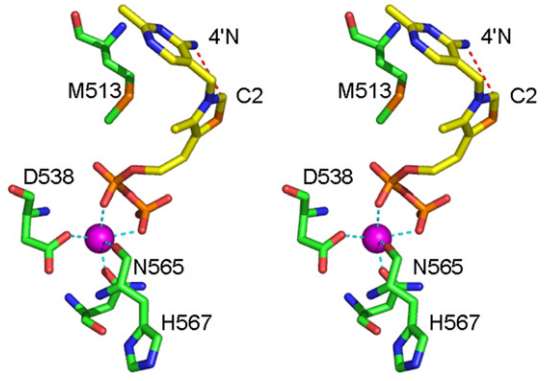

Fig. 7. Stereodiagram of the structure of ThDP when bound to the catalytic subunit of *A. thaliana* AHAS in complex with IQ. The pyrimidine and thiazolium rings are bent in a V conformation such that the 4′ nitrogen atom and the C2 carbon atom are 3.2 Å apart. In this structure Mg^{2+} is coordinated to five ligands.

There are several other conserved features of ThDP when bound to AHAS. With ThDP in the V-conformation, a close approach (3.3 Å in *A. thaliana* AHAS and 3.1 Å in the yeast AHAS) is made between the 4′N and C2 atoms (Fig. 7). Hydrogen bonds are always observed between a glutamate (E144 in *A. thaliana* AHAS) and the N1′ atom of ThDP and between the N4′ atom of ThDP and a backbone oxygen atom (G511 in *A. thaliana* AHAS). Collectively these interactions and the bending of ThDP favour the deprotonation of the C2 atom resulting in the reactive ylide species that initiates catalysis.

3.4. Mg^{2+}-binding site

AHAS requires a metal ion for catalytic activity but the enzyme does not exhibit a high level of specificity. *Salmonella typhimurium* AHASII is active in the presence of Mn^{2+}, Mg^{2+}, Ca^{2+}, Cd^{2+}, Co^{2+}, Zn^{2+}, Cu^{2+}, Al^{3+}, Ba^{2+} or Ni^{2+}[67]. The activity is about 50% for Ni^{2+} and 133% for Mn^{2+} as compared to Mg^{2+}. All of the other metals show activities within this range. The only role of the metal ion is to anchor the ThDP to the polypeptide. In all of the crystal structures of AHAS it is assumed that the metal ion observed in the structure is Mg^{2+} since it was added in high concentration (>5 mM) to the crystallization buffer and to the protein during purification.

In the *A. thaliana* AHAS structure with bound IQ, Mg^{2+} is five coordinate, with two of the ligands provided by the oxygen atoms of the diphosphate of ThDP and three of the ligands provided by polypeptide (Fig. 7). One of these ligands is the carbonyl oxygen atom of H567 and the other ligands are the side-chains of D538 and N565. The five ligands take positions that equate to distorted square pyramidal geometry, with the two diphosphate oxygens and two side-chain ligands forming the base of the pyramid and the carbonyl oxygen at the apex. In the structures where a sulfonylurea is bound the Mg^{2+}-binding site is different. In these structures, the metal ion is six coordinate, with the final ligand position filled by a water molecule. The overall geometry is best described as distorted octahedral. Thus, the binding of the different classes of herbicide appear to influence the way in which the Mg^{2+}- ion is held in place to the polypeptide. One explanation is that destruction of the thiazolium ring in the sulfonylurea structures has led to the relaxation of the Mg^{2+}-binding site.

3.5. FAD-binding site

In *A. thaliana* AHAS, FAD is bound tightly to the polypeptide with a K_m value of 1.5 μM [5]. The crystal structures show that FAD adopts a fully extended conformation with the bulk of the interactions formed through contacts to the β-domain (Fig. 8). It is clear that the surface of the β-domain has evolved such that it can accommodate the FAD in a highly complementary manner with respect to both shape and charge. It is certain that FAD does not play a hidden role in catalysis, because the acetolactate-specific enzyme (ALS) from *K. pneumoniae* possesses ThDP-Mg^{2+} as part of its catalytic

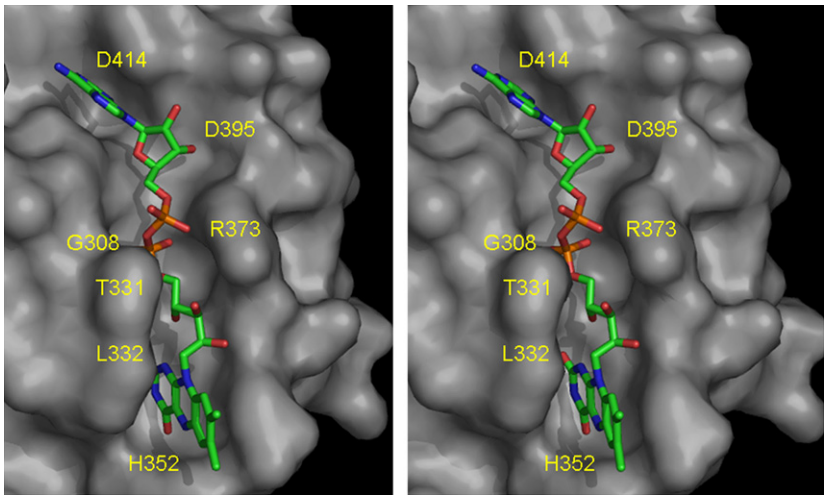

Fig. 8. Stereodiagram of the structure of FAD bound to the β-domain surface of the *A. thaliana* AHAS catalytic subunit as observed in the IQ complex. Residues from the β-domain that form polar contacts with the FAD are labelled. The extended conformation of FAD and the curvature of the isoalloxazine ring are observed in all of the *A. thaliana* AHAS and yeast AHAS structures.

machinery but is active without FAD. The crystal structure of this enzyme has also been determined [49] and it is similar to that of AHAS except for the groove that accommodates FAD in AHAS, which is filled with amino acid side-chains in the *K. pneumoniae* protein.

In all of the *A. thaliana* AHAS structures the isoalloxazine ring exhibits a slight bend across the N5–N10 axis that is indistinguishable from that observed in pyruvate oxidase. In our original structure of free yeast AHAS we had suggested that the isoalloxazine ring was flat, but in subsequent structural studies of that enzyme where a herbicide is bound, there is a clear indication that the ring is also bent. We therefore suggest that our original interpretation of the shape of isoalloxazine ring in the free structure is not correct. It has now been shown that the FAD can act as an electron acceptor in a slow side-reaction catalysed by AHAS [65] and this is favoured if the isoalloxazine ring does indeed tend towards the bent structure that would be adopted after reduction to $FADH_2$.

4. Mechanism of inhibition

4.1. Herbicide-binding site

The sulfonylurea and imidazolinone herbicides bind within the substrate-access channel (Fig. 9) of both plant and yeast AHAS [40,41,51]. In this way, both classes of herbicide inhibit AHAS by blocking substrate access to the active site. The sulfonylureas are situated so that the substituted aromatic ring projects out toward the surface of the protein, while the heterocyclic ring points towards the active site. Likewise, the dihydroimidazolone ring of IQ is buried within the channel, leaving most of the quinoline ring exposed near the surface of the protein. The sulfonylureas are ~2 Å closer to the active site than IQ so that sulfonylureas bearing methoxy substituents on the heterocyclic ring come in contact with the C7 methyl group of the isoalloxazine ring of FAD. If the IQ structure is superimposed on to any of the sulfonylurea structures, as in Fig. 9, it is apparent that the two classes of herbicide bind to overlapping sites, thereby substantiating reports that suggest mutually exclusive binding of sulfonylureas and imidazolinones [13,57,60].

By crystallizing herbicide complexes of both yeast and plant AHAS, we expected to discover the location of the herbicide-binding site and to learn how the sulfonylureas and imidazolinones inhibit the enzyme. We hoped to learn why some inhibitors are better than others and to gain some understanding of the differences between the two enzymes. In particular,

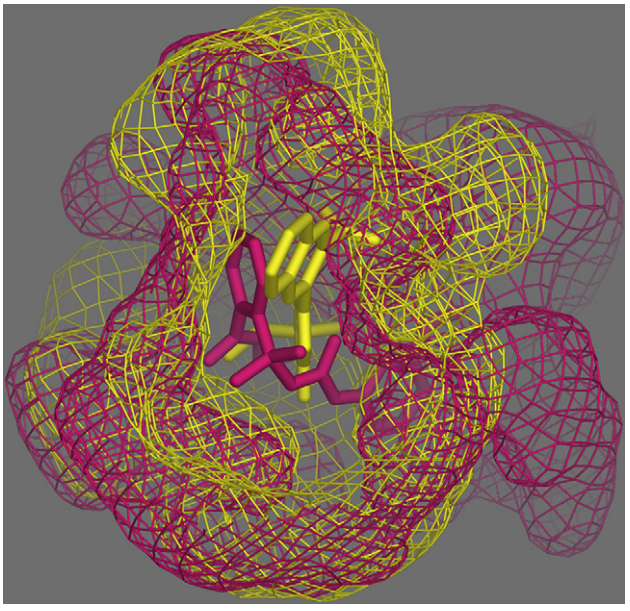

Fig. 9. Sulfonylurea and imidazolinone herbicides bind to overlapping sites in the substrate access channel of the catalytic subunit of AHAS. The substrate access channel (mesh contours) for CE-bound and IQ-bound (yellow mesh) *A. thaliana* AHAS have been overlaid and are contoured in pink and yellow mesh, respectively. CE and IQ are shown as pink and yellow stick representations, respectively.

we wanted to answer the following questions. What factors contribute to variations in the potency of different sulfonylureas? Is the methyl group substitution of the sulfonylurea bridge in TB responsible for it being a weaker inhibitor of both enzymes? Why is imazethapyr (IT) a much weaker inhibitor of plant AHAS than IQ? What makes sulfonylureas equally good inhibitors of both yeast and plant AHAS, while imidazolinones are far better inhibitors of the plant enzymes? On a similar note, why are sulfonylureas better inhibitors of any AHAS than the imidazolinones? Due to their weak binding to yeast AHAS it has not yet been possible to crystallize this enzyme in the presence of an imidazolinone herbicide; however, we were successful in crystallizing both enzymes with each of five sulfonylureas as well as the plant enzyme in complex with IQ.

All of the sulfonylureas crystallized with yeast and plant AHAS adopt the same overall conformation, as illustrated by CE in Fig. 10A, although the position of the aromatic ring with respect to the sulfonylurea bridge varies somewhat. For example, in comparison to that of CE bound to plant AHAS, the *ortho*-chlorobenzene ring of CS is shifted ~1 Å closer to the groove that normally binds the larger ethyl carboxyester *ortho* substituents. All of the sulfonylureas are very strong inhibitors of plant AHAS [6,68] and this potency can be attributed largely to all of the sulfonylureas making many of the same contacts with neighbouring amino acid residues. For example, V196, P197, M200, A205, and D376 are all involved in anchoring the aromatic ring through hydrophobic interactions, whereas the guanidinium group of R377 is hydrogen-bonded to at least one of the sulfonyl oxygen atoms, a nitrogen atom within the heterocyclic ring, and the methoxy substituent on the heterocyclic ring (Fig. 10A). Probably the single most important residue for binding any of the sulfonylurea herbicides is W574, for which the indole ring stacks on to the heterocyclic ring with an average distance of 3.5 Å (Fig. 10A). Of the 16 amino acid residues involved in sulfonylurea binding to plant AHAS, only four of these (R199, M200, K256, S653) adopt different conformations depending on which sulfonylurea is bound (Fig. 11A). R199 and M200 do not contact any of the sulfonylureas directly, and are presumably in different conformations within each structure simply because both residues are at the surface of the pocket and have some degree of flexibility. The terminal amino group of K256 adopts one conformation when hydrogen-bonded to either a sulfonyl oxygen atom of CE or to the adjacent NH group of SM or MM, and another conformation when a hydrogen bond is not made, as is the case for CS and TB. Due to the orientation of the aromatic ring of CS, and the presence of the methyl substituent on the sulfonylurea bridge of TB, K256 cannot hydrogen bond with either herbicide because the sulfonylurea oxygen and adjacent nitrogen atoms are slightly further away from K256 than for other sulfonylureas. Likewise, S653 adopts one of two conformations, depending on the number of hydrogen bonds made with the herbicide. For example, the β-hydroxyl group of S653 is hydrogen-bonded to oxygen atoms of both the sulfonyl and carbonyl groups in the sulfonylurea bridge of CE and SM, but only to the carbonyl oxygen

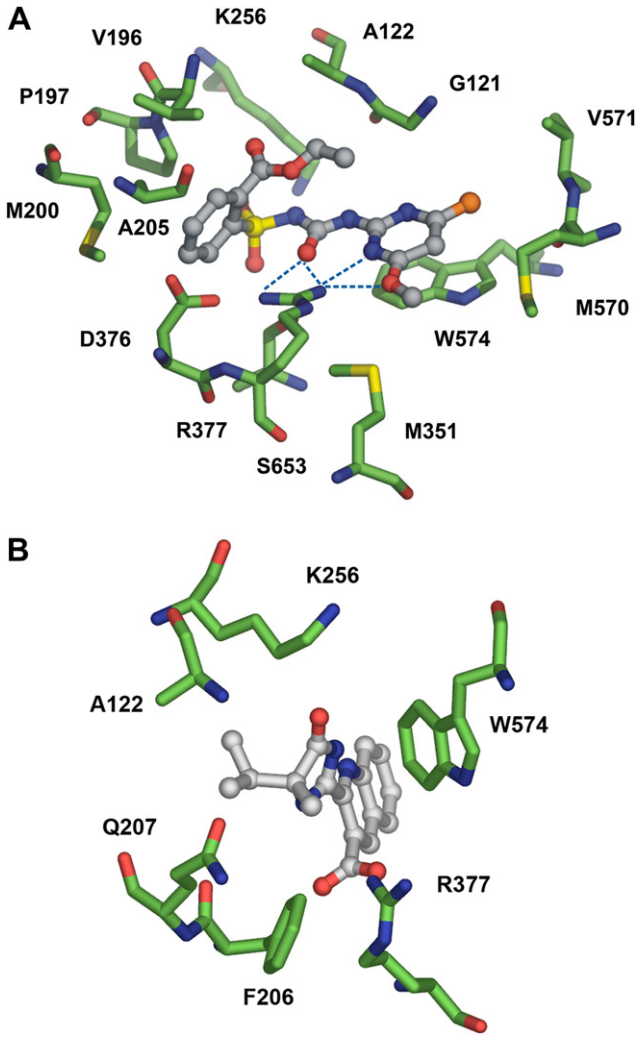

Fig. 10. Partial view of AHAS residues involved in herbicide binding. (A) The herbicide CE is shown as a ball-and-stick model with grey carbon atoms. Amino acid residues that interact with CE are shown as sticks models with green carbon atoms. Sulfur is yellow, oxygen red, nitrogen blue and chlorine orange. Hydrogen bonds are illustrated in blue as broken lines. Residues F206, Q207 and the hydrogen bond between S653 and CE are not shown. (B) The herbicide IQ is shown as a ball-and-stick model with grey carbon atoms. Amino acid residues that interact with IQ are represented as sticks with green carbon atoms. The colour scheme for other atoms is shown in (A). Residues R199, M200, M351, D376, S653, G654, and the hydrogen bond/salt bridge between R377 and the carboxylate moiety of IQ, are not shown.

atom of TB, MM, and CS, although there is no obvious structural reason for adopting one conformation over the other.

Examination of the crystal structures and the extensive characterization of 79 sulfonylurea inhibitors [68] suggest that some structural features are preferred over others. The best inhibitors of plant AHAS are sulfonylureas bearing larger *ortho* substituents on the aromatic ring (such as carboxy methyl or ethyl esters), in combination with either a classical sulfonylurea bridge, or one that is slightly longer (e.g. bensulfuron methyl or ethoxysulfuron), together with a heterocyclic ring bearing a small substituent on at least one (but preferably both) *meta* positions. This combination of features results in a snug fit within the active site tunnel (Fig. 12) and strong

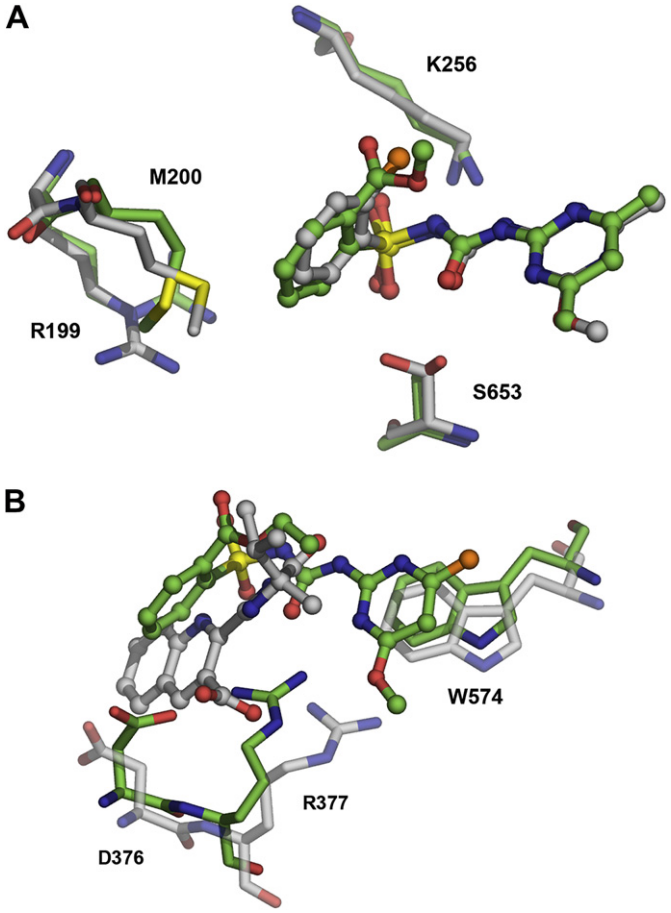

Fig. 11. Structural adjustments that accommodate different herbicides. (A) The orientation of three amino acid residues change depending on the type of sulfonylurea bound to AHAS. The herbicides are shown as ball-and-stick models. Carbon is coloured grey for CS or green for SM and the corresponding residues surrounding each herbicide, respectively. The colour scheme for other atoms is the same as Fig. 10A. (B) Conformational adjustments of three amino acid residues involved in binding IQ and sulfonylureas. Both herbicides are represented as ball-and-stick models; the residues surrounding IQ are shown as partially transparent. Carbon is coloured grey for IQ and green for CE and the residues surrounding each herbicide, respectively. The colour scheme for other atoms is the same as Fig. 10A.

interactions with nearby amino acids. Not only do sulfonylureas make numerous (>50) hydrophobic contacts with surrounding residues, but several key amino acids, such as K256, R377, and S653 are involved in making up to five hydrogen bonds with any of the five classical sulfonylureas crystallized. The most critical of these are probably the hydrogen bonds between R377, a residue that is crucial for catalysis [15,38], and atoms of the sulfonylurea bridge (Fig. 10A).

The herbicidally-active (*R*) enantiomer of IQ is bound to plant AHAS [41] through extensive interactions with 12 amino acid residues, most of which are hydrophobic. All but two of these residues, G654 and R199, are also involved in binding sulfonylureas. The carboxylate group that is present on all commercial imidazolinones makes a key ionic interaction with the side-chain of R377 (Fig. 10B). The methyl and isopropyl substituents of the dihydroimidazolone ring, which are required for herbicidal activity [37,63], are anchored to

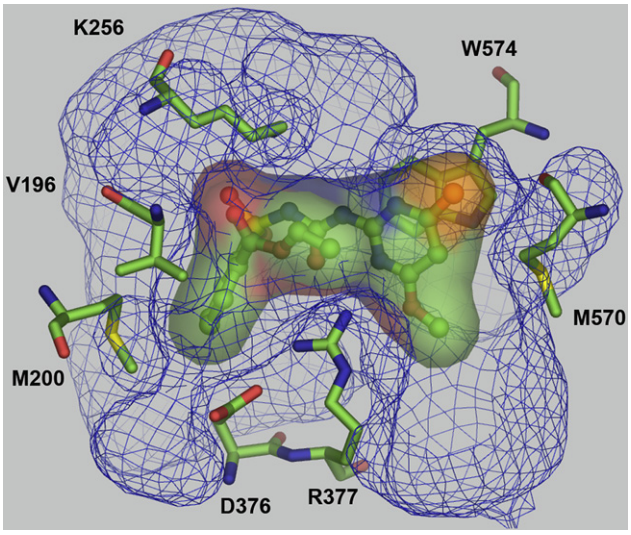

Fig. 12. The overall conformation of CE complements the shape of the herbicide-binding site. CE is represented by a ball-and-stick model and the molecular surface is shown. The herbicide-binding pocket is outlined in blue mesh. Select amino acid residues of the herbicide-binding site are represented by sticks. Carbon is coloured green; the colour scheme for other atoms is shown in Fig. 10A.

the enzyme through contacts with A122, F206, Q207, K256 and W574; the dihydroimidazolone ring itself contacts K256 and W574 (Fig. 10B). The rest of the molecule is packed rather loosely into the substrate access tunnel so that the large quinoline ring, a unique feature of IQ, actually protrudes through the mouth of the opening (Fig. 9). Nevertheless, it is easy to see that this functional group can make contacts with AHAS that would be absent for IP (which has the smaller pyridine ring), or reduced for IT (which has an ethyl-substituted the pyridine ring). This provides an explanation as to why IQ is a better inhibitor than other imidazolinones [6].

In general, the herbicide-binding sites in yeast and plant AHAS are similar; however two important differences could together account for the much weaker binding of imidazolinones to yeast AHAS. First of all, in plant AHAS the loop containing S653 is 3 Å closer to the herbicides than the corresponding residue G657 in yeast AHAS. Not only does the mutation G657S in yeast AHAS increase sensitivity to imidazolinones [12], but mutation of S653 in plants AHAS has been shown to give rise to imidazolinone resistance in the plant enzyme and in many plant species carrying this variant [19,56]. The second difference is that R199 in plant AHAS, which is believed to be functional in guiding imidazolinones into the binding site [24], is replaced by S194 in AHAS from yeast and several other species [11]. Our laboratory has demonstrated that, contrary to expectations, the yeast AHAS S194R mutant does not exhibit increased sensitivity to the imidazolinones. One reason for this may be that the residues on either side of R199 (R198 and M200) are needed to maintain the correct orientation of the arginine for imidazolinone binding; in yeast AHAS, the residues flanking S194 are T193 and A195.

Sulfonylurea- and imidazolinone-binding sites in plant AHAS are overlapping, and share ten amino acid residues.

A comparison of the residues involved in binding CE and IQ show that five of these adopt different conformations to accommodate the two classes of herbicide [41]. As mentioned previously, two of these residues (R199 and M200) have some rotational freedom that is evident even when different sulfonylureas are bound. The most striking differences in conformation are exhibited by D376, R377 and W574, which clearly adapt to bind one herbicide class over the other (Fig. 11B) [41]. For example, in the sulfonylurea structures D376 and R377 can easily form a salt bridge. However, in the IQ structure the quinoline ring wedges between these two amino acids forcing them apart with R377 rotating back and away from D376 to establish an ionic interaction with the carboxylate moiety of IQ. The same conformation of W574 observed in the IQ structure would impair binding of CE because it would protrude into the space occupied by the heterocyclic ring.

Although the field application rates of imidazolinone and sulfonylurea herbicides are similar, the sulfonylureas are much better inhibitors of AHAS than the imidazolinones. In general, inhibition constants for the imidazolinones are in the μM range, while those for the sulfonylureas are in the nM range [6,11]. This is probably because the overall shape and size of the sulfonylureas allow for a better fit, deeper into the tunnel, resulting in many more contacts than the imidazolinones. In addition, the sulfonylureas are anchored by at least five hydrogen bonds to three residues while IQ makes only one hydrogen bond, with R377.

4.2. Herbicide-resistant mutants

An astonishing number of weeds around the world today are resistant to AHAS inhibitors [66] and this resistance is usually caused by the sustained application of herbicides from a single class over several (4–7) consecutive growing seasons [28]. AHAS inhibitor resistance is either a consequence of enhanced metabolism of the herbicide by the plant or it is due to mutation of the AHAS gene, which in turn results in the change of a single amino acid residue in the herbicide-binding site [66]. At least 17 amino acid residues have been identified in bacteria, fungi, or plants where mutation results in herbicide resistance (Table 1). Herbicide-resistant AHAS mutants that have been catalogued include both natural isolates from resistant organisms and those that have been introduced intentionally in the laboratory. In both whole plants, and at the molecular level, mutations can lead to cross-tolerance among AHAS inhibitors. Cross-tolerance generally exists between sulfonylureas and triazolopyrimidines, or between imidazolinones and pyrimidyl(oxy/thio)benzoates; however some mutations result in broad cross-resistance to all four classes of herbicide [66].

AHAS inhibitors have been revolutionary to the herbicide market because they are potent, effective, and environmentally safe. In the face of an increasing number of weeds developing resistance, which might eventually destroy the usefulness of these herbicides, it is important to gain an understanding of AHAS resistance at the molecular level. This will facilitate the rational design of new herbicides and aid in the selection or engineering of herbicide-tolerant crops for the future [64,68]. The crystal structures of plant AHAS in complex with herbicides now enables us to make reasonable predictions on how a given mutation might impact on herbicide binding.

Almost all of the residues that surround and contribute to the binding of the five classical sulfonylureas crystallized in complex with plant AHAS have been implicated in herbicide resistance. Examination of these crystal structures has helped to explain the impact that various mutations have on sulfonylurea binding, and we have discussed some of these in the past [41]. However, some caution is needed in making such predictions. It is clear from the comparison between free and sulfonylurea-bound yeast AHAS (Fig. 6) that substantial structural changes take place when herbicides bind. Moreover, the changes that occur depend on the herbicide class, as revealed by comparing *A. thaliana* AHAS with bound IQ or sulfonylureas (Fig. 11B). Even different sulfonylureas cause small but significant structural perturbations (Fig. 11A). This flexibility of the protein implies that the effects of mutations on herbicide binding may not be revealed accurately by simply modelling the altered side-chain into the wild-type structure. Therefore, understanding how various AHAS mutations result in herbicide resistance is necessarily somewhat speculative.

Mutations of W574 that give rise to strong resistance to all four classes of herbicide are well documented (see Table 1). There are extensive interactions between W574 and the heterocyclic ring of sulfonylureas and so mutation of this residue to any other would necessarily result in the loss of many contacts. In addition, mutation of W574 would alter the contour of the herbicide-binding site, resulting in a less complementary fit for sulfonylurea herbicides. Similarly, mutation of any one of G121, M124, M570, or V571 which are clustered around the heterocyclic ring, or A122, P197, A205, or D376 which either anchor the aromatic ring or are located near its *ortho* substituent, would also effect sulfonylurea binding and result in resistance to this class of herbicide. Certainly, mutations of A122 [16], P197 [27], A205 [16], and W574 [2, 66] have been described in sulfonylurea-resistant organisms, although mutations of A122 are more commonly associated with imidazolinone resistance [11,66].

Other mutations (Table 1) that give rise to sulfonylurea resistance are not so easily explained. For example, H352 and D375 do not make contact with any of the five sulfonylureas crystallized with either plant AHAS or yeast AHAS, and F578 is not even within close proximity of any sulfonylurea! Presumably, the impact of these mutations is due to the effect on other nearby residues that are involved directly in herbicide binding. Unexpectedly, mutation of S653, which is usually involved in hydrogen bonding with sulfonylureas, is associated with resistance to imidazolinones rather than to sulfonylureas [11,66]. While it can be expected that conservative mutations such as S653T do not result in sulfonylurea resistance [2], it is not so clear why S653N mutants also remain sensitive to sulfonylureas [19,21]. The more radical S653F mutation does impact on sulfonylurea inhibition, although not as strongly as on that of imidazolinones [33].

Table 1
Herbicide-resistant mutations of AHAS

Residue in *A. thaliana*	Organism	Mutation	Resistance to herbicide class	Reference
G121	Yeast	G116[NS]	SU	[16]
	Yeast	G116S	SU/IM	[12]
A122	Yeast	A117[DEFHIKLMNPQRSTVWY]	SU	[16]
	Yeast	A117V	SU^R/IM^S	[12]
	A. thaliana	A122V	SU^S/IM^R	[6]
	E. coli	A26V	SU	[23]
	Tobacco	A121T	$SU^R/IM^R/TP^S$	[8]
	Cocklebur	A100T	SU^S/IM^R	[2]
M124	*A. thaliana*	M124E	SU/IM	[45]
V196	*E. coli*	V99M	SU^R/IM^S	[23]
P197	*A. thaliana*	P197S	SU	[20]
	Yeast	P192[AELQRSVWY]	SU	[16]
	Redroot pigweed	P197L	SU/IM/TP/PSB	[61]
R199	*A. thaliana*	R199E	SU^S/IM^R	[45]
A205	Yeast	A200[CDERTVWY]	SU	[16]
	Yeast	A200V	SU/IM	[12]
	E. coli	A108V	SU^R/IM^S	[23]
	Sunflower	A205V	IM	[27]
K256	Yeast	K251[DENPT]	SU	[16]
	Yeast	K251T	SU/IM	[12]
	Tobacco	K255[FQ]	SU/IM/TP	[69]
M351	Yeast	M354[CKV]	SU	[16]
	Yeast	M354V	SU^R/IM^S	[12]
	Tobacco	M350C	SU/IM/TP	[30]
H352	Tobacco	H351Q	SU/IM/TP	[44]
D375	Tobacco	D374A	SU/IM	[32]
D376	Tobacco	D375[AE]	SU/TP	[32]
	Yeast	D379N	SU^R/IM^S	[12]
	Yeast	D379[EGNPSVW]	SU	[16]
M570	*E. coli*	M460N	SU	[24]
	Tobacco	M569C	SU/IM/TP	[30]
V571	Yeast	V583[ACNY]	SU	[16]
	Yeast	V583A	SU^R/IM^S	[12]
	Tobacco	V570Q	SU/TP	[25]
W574	Yeast	W586[ACEGHIKLNSV]	SU	[16]
	Yeast	W586L	SU/IM	[12]
	E. coli	W464[AFLQY]	SU	[24]
	A. thaliana	W574[LS]	SU/IM	[6]
	Oilseed rape	W557L	SU/IM/TP	[18]
	Cocklebur	W552L	SU/IM/TP/POB	[2]
	Cotton	W563[CS]	SU/IM	[54]
F578	Yeast	F590[CGLNR]	SU	[16]
	Yeast	F590L	SU/IM	[12]
	Tobacco	F577[DE]	SU/IM/TP	[25]
S653	*A. thaliana*	S653N	IM	[56]
	A. thaliana	S653T	SU^S/IM^R	[33]
	A. thaliana	S653F	SU/IM	[33]
	A. thaliana	S653N	SU^S/IM^R	[6]
	Tobacco	S652T	SU^S/IM^R/ TP^S	[8]

Herbicide "resistance" is only reported for mutant enzymes with ≥10-fold increases in the inhibition constant (K_i^{app}, IC_{50}) relative to the wild-type enzyme. Resistant^R and sensitive^S types are indicated in cases where one or more class of herbicide was tested but resistance was only evident for one class. Herbicide classes are abbreviated: SU, sulfonylurea; IM, imidazolinone; TP, triazolopyrimidine; POB, pyrimidyloxybenzoate; PSB, pyrimidylthiobenzoate.

Most imidazolinones that are currently on the market are similar in structure (Fig. 3), consisting of a carboxylated aromatic ring (typically pyridine) linked to a dihydroimidazolone ring with geminal methyl and isopropyl substituents. Often the aromatic ring is substituted in the *para* position relative to the dihydroimidazolone ring; IQ is unusual because its aromatic ring is a quinoline. Mutations to amino acid residues that are involved in anchoring the disubstituted dihydroimidazolone ring (A122, F206, Q207, K256, W574, and S653), or the carboxylated aromatic ring (M200, M351, D376, or G654), would be expected to weaken the binding of this class of herbicide to AHAS. However, only five (A122, K256, M351, W574, and S653; see Table 1) of the 12 residues that bind IQ have been implicated in resistance to this class of herbicide. Interestingly, there have not yet been reports of herbicide-resistant mutants for several residues that appear to be important

for imidazolinone binding (V196, M200, F206, and Q207). In contrast, some imidazolinone-resistant mutations have been identified for residues which appear to have no direct function in binding IQ whatsoever (M124, A205, H352, D375, M570, V571; see Table 1).

It is well documented that mutations of A122, W574, and S653 impart strong resistance to imidazolinones [6,8,19,33,56,66]. Both A122 and W574 make important hydrophobic contacts with IQ and mutation of A122 to a larger, or polar, residue would almost certainly result in repositioning of the herbicide. Similarly, if W574 were mutated to almost any other residue, important hydrophobic contacts with IQ would be lost. In addition, as mentioned previously for sulfonylurea herbicides, W574 is a key residue for defining the shape of the substrate access tunnel so that its mutation to another residue is expected to weaken imidazolinone binding drastically. The side-chain of S653 flanks the dihydroimidazolone ring of IQ and is adjacent to W574. Due to steric constraints, substitution of S653 to anything larger than serine, such as asparagine or threonine (see Table 1), is also likely to interfere with IQ binding.

Although G121 and P197 do not contact IQ directly, mutation of these residues [12,61] can also result in imidazolinone resistance. Due to its close proximity to the isopropyl moiety, mutation of G121 to any other residue is unlikely to be tolerated because the side-chain would protrude into the imidazolinone-binding site. Similarly, although mutation of the adjacent residue in space (S168) has never been linked to imidazolinone resistance, residues larger than serine are also expected to impair imidazolinone binding. Depending on the substitution, mutation of P197 gives rise to broad cross-tolerance among imidazolinones, sulfonylureas, triazolopyrimidines, and pyrimidyl(oxy/thio)benzoates (see Table 1). Although P197 is not involved in binding IQ, substitution to a bulky amino acid would obstruct its entry into the tunnel.

It is interesting that resistance has developed so rapidly among plants exposed to AHAS-inhibiting herbicides and moreover, the number of mutations that give rise to herbicide resistance is astounding. In the next section, we discuss the conservation of the herbicide-binding site throughout evolution and explain how plants are able to survive despite these mutations in an enzyme which is critical for the synthesis of branched-chain amino acids.

5. Conservation and function of the herbicide-binding site

When bound to *A. thaliana* AHAS, CE makes contact with 16 amino acids. Of these, 14 are completely conserved in yeast AHAS and there is only one further difference in *E. coli* AHASII. This cannot be due purely to chance because the overall amino acid sequence identity across the three proteins is less than 30%; on probability alone, approximately five conserved residues only would be expected. Clearly the residues comprising the herbicide-binding site have been maintained through the two billion years since eukaryotes and bacteria shared a common ancestor.

For some of these amino acids, conservation is necessary to maintain catalytic activity. The best example of this is R377. This residue is suggested to bind to the carboxylate of one or both substrates, and mutation of the corresponding residue to phenylalanine in tobacco AHAS [31] abolishes activity. Moreover, mutation of the equivalent residue in *E. coli* AHASII [15] points to a critical role for this arginine in the stabilization of the hydroxyethyl-ThDP and/or the breaking of the product–ThDP bond. R377 is in contact with F206 and mutation of the equivalent phenylalanine in *E. coli* AHASII [15] drastically reduces activity.

The conservation of other residues can be explained by more subtle effects. For example, mutation of W574 has relatively minor effects on the activity and kinetic properties of *A. thaliana* AHAS [6]. However, this residue is important in maintaining the preference for 2-ketobutyrate as the second substrate [24] so mutation would be selected against because of the potential for a resultant isoleucine starvation. Nevertheless, this defect is clearly not fatal for plants because changes to W574 are amongst the most commonly observed herbicide-resistant mutations in the field. If an AHAS mutation is observed in a viable organism then clearly this variant enzyme must remain functional. Indeed, of the 13 totally conserved contact residues mentioned above, only three (F206, Q207 and R377) are not found in herbicide-resistant organisms (Table 1). As mentioned above, F206 and R377 are essential for activity so their conservation is to be expected. As far as we are aware, no Q207 mutants have been constructed or isolated from natural sources, although several papers have noted its proximity to the active site [7,23,24,49]. We predict that mutating this residue would result in a major reduction of AHAS activity. The remaining ten residues appear to have been conserved for the sole function of binding herbicides! Clearly this is an absurd proposition and highlights a major gap in our knowledge. What are the natural functions of the residues involved in herbicide binding? We have no clear answer to this question but encourage others to develop testable theories.

Acknowledgements

We would like to thank Dr Renaud Dumas for giving us the opportunity to contribute this review.

References

[1] L.M. Abell, J.V. Schloss, Oxygenase side reactions of acetolactate synthase and other carbanion-forming enzymes, Biochemistry 30 (1991) 7883–7887.
[2] P. Bernasconi, A.R. Woodworth, B.A. Rosen, M.V. Subramanian, A naturally occurring point mutation confers broad range tolerance to herbicides that target acetolactate synthase, J. Biol. Chem. 270 (1995) 17381–17385.
[3] W.P. Burmeister, Structural changes in cryo-cooled protein crystals owing to radiation damage, Acta Crystallogr. D56 (2000) 328–341.
[4] R.S. Chaleff, C.J. Mauvais, Acetolactate synthase is the site action of two sulfonylurea herbicides in higher plants, Science 224 (1984) 1443–1445.
[5] A.K. Chang, R.G. Duggleby, Expression, purification and characterization of *Arabidopsis thaliana* acetohydroxyacid synthase, Biochem. J. 327 (1997) 161–169.

[6] A.K. Chang, R.G. Duggleby, Herbicide-resistant forms of *Arabidopsis thaliana* acetohydroxyacid synthase: characterization of the catalytic properties and sensitivity to inhibitors of four defined mutants, Biochem. J. 333 (1998) 765–777.
[7] D.M. Chipman, R.G. Duggleby, K. Tittmann, Mechanisms of acetohydroxyacid synthases, Curr. Opin. Chem. Biol. 9 (2005) 475–481.
[8] C.K. Chong, J.D. Choi, Amino acid residues conferring herbicide tolerance in tobacco acetolactate synthase, Biochem. Biophys. Res. Commun. 279 (2000) 462–467.
[9] D. Dobritzsch, S. Konig, G. Schneider, G. Lu, High resolution crystal structure of pyruvate decarboxylase from *Zymomonas mobili*s. Implications for substrate activation in pyruvate decarboxylases, J. Biol. Chem. 273 (1998) 20196–20204.
[10] R.G. Duggleby, Domain relationships in thiamine diphosphate-dependent enzymes, Acc. Chem. Res. 39 (2006) 550–557.
[11] R.G. Duggleby, S.S. Pang, Acetohydroxyacid synthase, J. Biochem. Mol. Biol. 33 (2000) 1–36.
[12] R.G. Duggleby, S.S. Pang, H. Yu, L.W. Guddat, Systematic characterization of mutations in yeast acetohydroxyacid synthase: interpretation of herbicide-resistance data, Eur. J. Biochem. 270 (2003) 2895–2904.
[13] J. Durner, V. Gailus, P. Böger, New aspects on inhibition of plant acetolactate synthase by chlorsulfuron and imazaquin, Plant Physiol. 95 (1991) 1144–1149.
[14] F. Dyda, W. Furey, S. Swaminathan, M. Sax, B. Farrenkopf, F. Jordan, Catalytic centers in the thiamine diphosphate dependent enzyme pyruvate decarboxylase at 2.4-Å resolution, Biochemistry 32 (1993) 6165–6170.
[15] S. Engel, M. Vyazmensky, M. Vinogradov, D. Berkovich, A. Bar-Ilan, U. Qimron, Y. Rosiansky, Z. Barak, D. Chipman, Role of a conserved arginine in the mechanism of acetohydroxyacid synthase, J. Biol. Chem. 279 (2004) 24803–24812.
[16] S.C. Falco, R.E. McDevitt, C.-F. Chui, M.E. Hartnett, S. Knowlton, C.J. Mauvais, J.K. Smith, B.J. Mazur, Engineering herbicide-resistant acetolactate synthase, Dev. Ind. Microbiol. 30 (1989) 187–194.
[17] M.S. Hasson, A. Muscate, M.J. Mcleish, L.S. Polovnikova, J.A. Gerlt, G.L. Kenyon, G.A. Petsko, D. Ringe, The crystal structure of benzoylformate decarboxylase at 1.6 Å resolution: diversity of catalytic residues in thiamine diphosphate-dependent enzymes, Biochemistry 37 (1998) 9918–9930.
[18] J. Hattori, D. Brown, G. Mourad, H. Labbé, T. Ouellet, G. Sunohara, R. Rutledge, J. King, B. Miki, An acetohydroxy acid synthase mutant reveals a single site involved in multiple herbicide resistance, Mol. Gen. Genet. 246 (1995) 419–425.
[19] J. Hattori, R. Rutledge, H. Labbé, D. Brown, G. Sunohara, B. Miki, Multiple resistance to sulfonylureas and imidazolinones conferred by an acetohydroxyacid synthase gene with separate mutations for selective resistance, Mol. Gen. Genet. 232 (1992) 167–173.
[20] G.W. Haughn, J. Smith, B. Mazur, C. Somerville, Transformation with a mutant *Arabidopsis* acetolactate synthase gene renders tobacco resistant to sulfonylurea herbicides, Mol. Gen. Genet. 211 (1988) 266–271.
[21] G.W. Haughn, C. Somerville, A mutation causing imidazolinone resistance maps to the *Csr1* locus of *Arabidopsis thaliana*, Plant Physiol. 92 (1990) 1081–1085.
[22] H.P. Hershey, L.J. Schwartz, J.P. Gale, L.M. Abell, Cloning and functional expression of the small subunit of acetolactate synthase from *Nicotiana plumbaginifolia*, Plant Mol. Biol. 40 (1999) 795–806.
[23] C.M. Hill, R.G. Duggleby, Mutagenesis of *Escherichia coli* acetohydroxyacid synthase isoenzyme II and characterization of three herbicide-insensitive forms, Biochem. J. 335 (1998) 653–661.
[24] M. Ibdah, A. Bar-Ilan, O. Livnah, J.V. Schloss, Z. Barak, D.M. Chipman, Homology modeling of the structure of bacterial acetohydroxy acid synthase and examination of the active site by site-directed mutagenesis, Biochemistry 35 (1996) 16282–16291.
[25] S.M. Jung, D.T. Le, S.S. Yoon, M.Y. Yoon, Y.T. Kim, J.D. Choi, Amino acid residues conferring herbicide resistance in tobacco acetohydroxy acid synthase, Biochem. J. 383 (2004) 53–61.
[26] A. Kaplun, M. Vyazmensky, Y. Zherdev, I. Belenky, A. Slutzker, S. Mendel, Z. Barak, D.M. Chipman, B. Shaanan, Structure of the regulatory subunit of acetohydroxyacid synthase isozyme III from *Escherichia coli*, J. Mol. Biol. 357 (2006) 951–963.
[27] J.M. Kolkman, M.B. Slabaugh, J.M. Bruniard, S. Berry, B.S. Bushman, C. Olungu, N. Maes, G. Abratti, A. Zambelli, J.F. Miller, A. Leon, S.J. Knapp, Acetohydroxyacid synthase mutations conferring resistance to imidazolinone or sulfonylurea herbicides in sunflower, Theor. Appl. Genet. 109 (2004) 1147–1159.
[28] Y.I. Kuk, K.H. Kim, O.D. Kwon, D.J. Lee, N.R. Burgos, S. Jung, J.O. Guh, Cross resistance pattern and alternative herbicides for *Cyperus difformis* resistant to sulfonylurea herbicides in Korea, Pest Manage. Sci. 60 (2004) 85–94.
[29] R.A. LaRossa, J.V. Schloss, The sulfonylurea herbicide sulfometuron methyl is an extremely potent and selective inhibitor of acetolactate synthase in *Salmonella typhimurium*, J. Biol. Chem. 259 (1984) 8753–8757.
[30] D.T. Le, M.Y. Yoon, Y.T. Kim, J.D. Choi, Roles of conserved methionine residues in tobacco acetolactate synthase, Biochim. Biophys. Res. Commun. 306 (2003) 1075–1082.
[31] D.T. Le, M.Y. Yoon, Y.T. Kim, J.D. Choi, Roles of three well-conserved arginine residues in mediating the catalytic activity of tobacco acetohydroxy acid synthase, J. Biochem. (Tokyo) 138 (2005) 35–40.
[32] D.T. Le, M.Y. Yoon, Y.T. Kim, J.D. Choi, Two consecutive aspartic acid residues conferring herbicide resistance in tobacco acetohydroxy acid synthase, Biochim. Biophys. Acta 1749 (2005) 103–112.
[33] Y.-T. Lee, A.K. Chang, R.G. Duggleby, Effect of mutagenesis at serine 653 of *Arabidopsis thaliana* acetohydroxyacid synthase on the sensitivity to imidazolinone and sulfonylurea herbicides, FEBS Lett. 452 (1999) 341–345.
[34] Y.-T. Lee, R.G. Duggleby, Identification of the regulatory subunit of *Arabidopsis thaliana* acetohydroxyacid synthase and reconstitution with its catalytic subunit, Biochemistry 40 (2001) 6836–6844.
[35] Y.-T. Lee, R.G. Duggleby, Mutations in the regulatory subunit of yeast acetohydroxyacid synthase affect its activation by MgATP, Biochem. J. 395 (2006) 331–336.
[36] G. Levitt, Herbicidal sulfonamides, US Patent 4127405 (1978).
[37] M. Los, *o*-(5-Oxo-2-imidazolin-2-yl)arylcarboxylates: a new class of herbicides, in: P.S. Magee, G.K. Kohn, J.J. Menn (Eds.), Pesticide Synthesis Through Rational Approaches, American Chemical Society, New York, 1984, pp. 29–44.
[38] J.A. McCourt, R.G. Duggleby, Acetohydroxyacid synthase and its role in the biosynthetic pathway for branched-chain amino acids, Amino Acids 31 (2006) 173–210.
[39] J.A. McCourt, P.F. Nixon, R.G. Duggleby, Thiamin nutrition and catalysis-induced instability of thiamin diphosphate, Br. J. Nutr. 96 (2006) 636–638.
[40] J.A. McCourt, S.S. Pang, R.G. Duggleby, L.W. Guddat, Elucidating the specificity of binding of sulfonylurea herbicides to acetohydroxyacid synthase, Biochemistry 44 (2005) 2330–2338.
[41] J.A. McCourt, S.S. Pang, J. King-Scott, R.G. Duggleby, L.W. Guddat, Herbicide binding sites revealed in the structure of *Arabidopsis thaliana* acetohydroxyacid synthase, Proc. Natl. Acad. Sci. USA 103 (2006) 569–573.
[42] S. Mendel, T. Elkayam, C. Sella, V. Vinogradov, M. Vyazmensky, D.M. Chipman, Z. Barak, Acetohydroxyacid synthase: a proposed structure for regulatory subunits supported by evidence from mutagenesis, J. Mol. Biol. 307 (2001) 465–477.
[43] Y.A. Muller, G.E. Schulz, Structure of the thiamine- and flavin-dependent enzyme pyruvate oxidase, Science 259 (1993) 965–967.
[44] K.J. Oh, E.J. Park, M.Y. Yoon, T.R. Han, J.D. Choi, Roles of histidine residues in tobacco acetolactate synthase, Biochem. Biophys. Res. Commun. 282 (2001) 1237–1243.
[45] K.H. Ott, J.-G. Kwagh, G.W. Stockton, V. Sidorov, G. Kakefuda, Rational molecular design and genetic engineering of herbicide resistant crops by structure modeling and site-directed mutagenesis of acetohydroxyacid synthase, J. Mol. Biol. 263 (1996) 359–368.
[46] S.S. Pang, R.G. Duggleby, Expression, purification, characterization, and reconstitution of the large and small subunits of yeast acetohydroxyacid synthase, Biochemistry 38 (1999) 5222–5231.

[47] S.S. Pang, R.G. Duggleby, Regulation of yeast acetohydroxyacid synthase by valine and ATP, Biochem. J. 357 (2001) 749–757.
[48] S.S. Pang, R.G. Duggleby, L.W. Guddat, Crystal structure of yeast acetohydroxyacid synthase: a target for herbicidal inhibitors, J. Mol. Biol. 317 (2002) 249–262.
[49] S.S. Pang, R.G. Duggleby, R.L. Schowen, L.W. Guddat, The crystal structures of *Klebsiella pneumoniae* acetolactate synthase with enzyme-bound cofactor and with an unusual intermediate, J. Biol. Chem. 279 (2004) 2242–2253.
[50] S.S. Pang, L.W. Guddat, R.G. Duggleby, Crystallization of the catalytic subunit of *Saccharomyces cerevisiae* acetohydroxyacid synthase, Acta Crystallogr. D57 (2001) 1321–1323.
[51] S.S. Pang, L.W. Guddat, R.G. Duggleby, Molecular basis of sulfonylurea herbicide inhibition of acetohydroxyacid synthase, J. Biol. Chem. 278 (2003) 7639–7644.
[52] S.S. Pang, L.W. Guddat, R.G. Duggleby, Crystallization of *Arabidopsis thaliana* acetohydroxyacid synthase in complex with the sulfonylurea herbicide chlorimuron ethyl, Acta Crystallogr. D60 (2004) 153–155.
[53] J.J. Petkowski, M. Chruszcz, M.D. Zimmerman, H. Zheng, T. Skarina, O. Onopriyenko, M.T. Cymborowski, K.D. Koclega, A. Savchenko, A. Edwards, W. Minor, Crystal structures of TM0549 and NE1324-two orthologs of *E. coli* AHAS isozyme III small regulatory subunit, Protein Sci. 16 (2007) 1360–1367.
[54] K. Rajasekaran, J.W. Grula, D.M. Anderson, Selection and characterization of mutant cotton (*Gossypium hirsutum* L.) cell lines resistant to sulfonylurea and imidazolinone herbicides, Plant Sci. 119 (1996) 115–124.
[55] T. Ray, Site of action of chlorsulfuron, Plant Physiol. 75 (1984) 827–831.
[56] K. Sathasivan, G.W. Haughn, N. Murai, Molecular basis of imidazolinone herbicide resistance in *Arabidopsis thaliana* var Columbia, Plant Physiol. 97 (1991) 1044–1050.
[57] J.V. Schloss, M. Ciskanik, D.E. Van Dyk, Origin of the herbicide binding site of acetolactate synthase, Nature 331 (1988) 360–362.
[58] J.V. Schloss, D.E. Van Dyk, J.F. Vasta, R.M. Kutny, Purification and properties of *Salmonella typhimurium* acetolactate synthase isozyme II from *Escherichia coli* HB101/pDU9, Biochemistry 24 (1985) 4952–4959.
[59] D.L. Shaner, P.C. Anderson, M.A. Stidham, Imidazolinones: potent inhibitors of acetohydroxyacid synthase, Plant Physiol. 76 (1984) 545–546.
[60] D.L. Shaner, B.K. Singh, M.A. Stidham, Interaction of imidazolinones with plant acetohydroxy acid synthase: evidence for *in vivo* binding and competition with sulfometuron methyl, J. Agric. Food Chem. 38 (1990) 1279–1282.
[61] M. Sibony, A. Michel, H.U. Haas, B. Rubin, K. Hurle, Sulfometuron-resistant *Amaranthus retroflexus*: cross resistance and molecular basis for resistance to acetolactate synthase-inhibiting herbicides, Weed Res. 41 (2001) 509–522.
[62] B.K. Singh, M.A. Stidham, D.L. Shaner, Assay of acetohydroxyacid synthase, Anal. Biochem. 171 (1988) 173–179.
[63] M.A. Stidham, B.K. Singh, Imidazolinone-acetohydroxyacid synthase interactions, in: D.L. Shaner, S.L. O'Connor (Eds.), The Imidazolinone Herbicides, CRC Press, Boca Raton, FL, 1991, pp. 71–90.
[64] S. Tan, R.R. Evans, M.L. Dahmer, B.K. Singh, D.L. Shaner, Imidazolinone-tolerant crops: history, current status and future, Pest Manage. Sci. 61 (2005) 246–257.
[65] K. Tittmann, K. Schroder, R. Golbik, J. McCourt, A. Kaplun, R.G. Duggleby, Z. Barak, D.M. Chipman, G. Hubner, Electron transfer in acetohydroxyacid synthase as a side reaction of catalysis. Implications for the reactivity and portioning of the carbanion/enamine form of (α-hydroxyethyl)thiamine diphosphate in a "nonredox" flavoenzyme, Biochemistry 43 (2004) 8652–8661.
[66] P.J. Tranel, T.R. Wright, Resistance to ALS-inhibiting herbicides: what have we learned? Weed Sci. 50 (2002) 700–712.
[67] J.M.-T. Tse, J.V. Schloss, The oxygenase reaction of acetolactate synthase, Biochemistry 32 (1988) 10398–10403.
[68] J.-G. Wang, Z.-M. Li, N. Ma, B.-L. Wang, L. Jiang, S.S. Pang, Y.-T. Lee, L.W. Guddat, R.G. Duggleby, Structure-activity relationships for a new family of sulfonylurea herbicides, J. Comput.-Aided Mol. Des. 19 (2005) 801–820.
[69] T.Y. Yoon, S.M. Chung, S.I. Chang, M.Y. Yoon, T.R. Hahn, J.D. Choi, Roles of lysine 219 and 255 residues in tobacco acetolactate synthase, Biochem. Biophys. Res. Commun. 293 (2002) 433–439.